Understanding volatility correlation behavior with a magnitude cross-correlation function

Woo Cheol Jun,* Gabjin Oh,† and Seunghwan Kim‡
Asia Pacific Center for Theoretical Physics, Department of Physics, Nonlinear Complex Systems Laboratory, POSTECH Pohang, Republic of Korea 790-784
(Received 8 November 2005; published 29 June 2006)

We propose an approach for analyzing the basic relation between correlation properties of the original signal and its magnitude fluctuations by decomposing the original signal into its positive and negative fluctuation components. We use this relation to understand the following phenomenon found in many naturally occurring time series: the magnitude of the signal exhibits long-range correlation, whereas the original signal is short-range correlated. The applications of our approach to heart rate variability signals and high-frequency foreign exchange rates reveal that the difference between the correlation properties of the original signal and its magnitude fluctuations is induced by the time organization structure of the correlation function between the magnitude fluctuations of positive and negative components. We show that this correlation function can be described well by a stretched-exponential function and is related to the nonlinearity and the multifractal structure of the signals.

DOI: 10.1103/PhysRevE.73.066128 PACS number(s): 89.65.Gh, 89.75.Da, 87.10.+e, 89.20.−a

I. INTRODUCTION

The study of diverse natural and nonstationary signals has recently become an area of active research for physicists [1–5]. This is because these signals exhibit interesting dynamical properties such as scale invariance, volatility correlation, heavy tails, and multifractality. Among these properties, empirical findings established volatility correlation behavior; the changes $x(t)$ $[=X(t+1)-X(t)]$ of a signal $[X(t)]$ are exponentially (short-range) correlated, while the magnitude series $|x(t)|$ is power-law (long-range) correlated [2–4]. Moreover, it was shown that the volatility correlation is universally observed in diverse time series including economic data, climate records, and medical signals, which can be used for economic prediction, climatic risk estimation, and clinical applications [2–4]. These studies provide strong empirical evidence for the existence of a certain relation between volatility correlation and nonlinearity of time series, and also show that the long-range correlation in the magnitude time series is related to the multifractal spectrum width of the signal. However, these findings are empirical and the exact relation between the correlation in $x(t)$ and the correlation in $|x(t)|$ is unknown. For example, it still remains unclear what structure of the original fluctuation signal generates volatility correlation behavior [5].

In this paper, we show that the relation between scaling behaviors of original signals and their magnitude fluctuations can be derived naturally from a detrended fluctuation analysis (DFA), which is a robust scaling analysis for quantifying correlation properties of natural signals [6].

We find that the volatility correlation behavior is induced by the correlation structure between magnitude fluctuations of positive and negative components in a fluctuating signal. Moreover, we confirm this relation by using a magnitude cross-correlation function, which describes the behavior of correlation between two magnitude signals for each time scale. We find that this magnitude cross-correlation function can be approximated well by a stretched-exponential function [7]. We then argue that signals with identical long-range correlations in their magnitude signals can exhibit different correlation properties depending on the time organization structures of the magnitude cross-correlation function. Our method is quite general and is applied to heart rate variability (HRV) signals and high-frequency foreign exchange (FX) rates [8] in this paper. We find that the magnitude cross-correlation function reflects the nonlinear properties and multifractal structures of these signals.

II. EXPLANATION OF THE VOLATILITY CORRELATION BEHAVIOR USING THE DFA METHOD

A. Analytical treatment

In our method, the original fluctuation signal $x(t)$ $(t=1,2,\ldots,N)$ is decomposed into two sign-separated components; a positive fluctuation signal $x_p(t)$ $[=x(t)$ if $x(t)>0$, 0 otherwise], and a negative fluctuation signal $x_n(t)$ $[=x(t)$ if $x(t)<0$, 0 otherwise]. Then, $x(t)=x_p(t)+x_n(t)$. In general, by the superposition rule of the detrended fluctuation analysis method in the reconstruction of the signal from the summation of two fluctuation signals $f(t)$ and $g(t)$, there exists a well-known mathematical relation between their root mean square (rms) fluctuation functions F_f, F_g, and F_{f+g} [9]. This can be applied to our case as follows:

$$F^2(n) = F_p^2(n) + F_n^2(n) + 2F_{pn}(n), \tag{1}$$

where $F(n)$, $F_p(n)$, and $F_n(n)$ are the rms fluctuations for segments with time length n of the cumulative integrated signals $Y(t)$, $Y_p(t)$, and $Y_n(t)$ for $x(t)$, $x_p(t)$, and $x_n(t)$, respectively.

Note that F_{pn} in Eq. (1) is represented as

*Electronic address: dalma21c@postech.ac.kr
†Electronic address: gq478051@postech.ac.kr
‡Electronic address: swan@postech.ac.kr

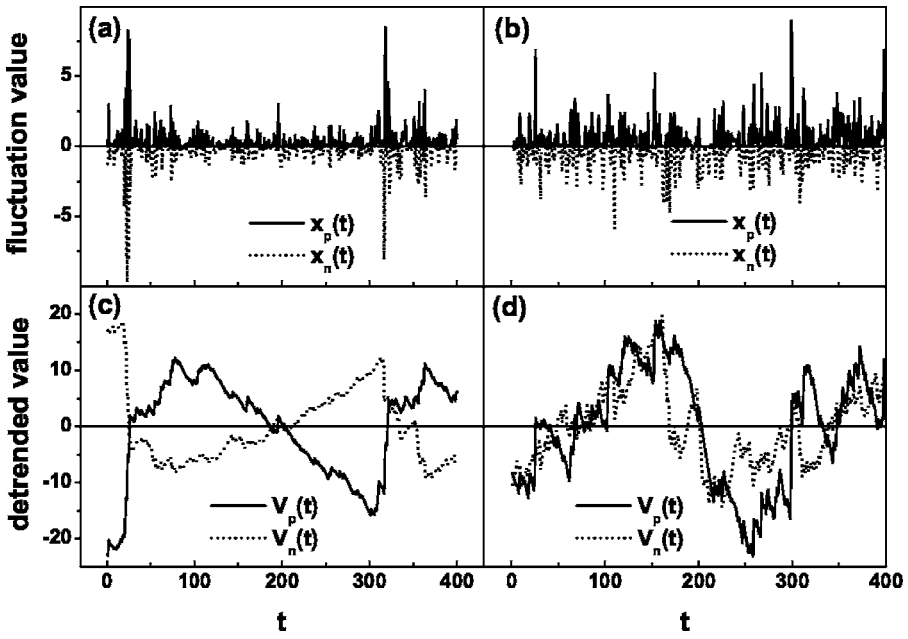

FIG. 1. (a) The fluctuation $x(t)$ for the out-of-phase correlated state in a segment υ of time length $n=400$. The solid (dotted) line corresponds to $x_p(t)$ $[x_n(t)]$ of $x(t)$. (b) The in-phase correlated state. (c) The vectors $\vec{V}_p^{\upsilon}$ (solid) of $x_p(t)$ and $\vec{V}_n^{\upsilon}$ (dotted) of $x_n(t)$ for $x(t)$ in (a). (d) $\vec{V}_p^{\upsilon}$ and $\vec{V}_n^{\upsilon}$ for $x(t)$ in (b). The data are from the FX exchange rate of lira (Italy) for the U.S. dollar in 1996 [8].

$$F_{pn}(n) = \frac{1}{2L_n}\sum_{\upsilon=1}^{2L_n}\left(\frac{1}{n}\sum_{t=1}^{n}[Y_p^{\upsilon}(t)-y_p^{\upsilon}(t)][Y_n^{\upsilon}(t)-y_n^{\upsilon}(t)]\right)$$
$$= \frac{1}{2L_n}\sum_{\upsilon=1}^{2L_n}\left(\frac{1}{n}|\vec{V}_p^{\upsilon}||\vec{V}_n^{\upsilon}|\cos(\theta_{pn}^{\upsilon})\right), \quad (2)$$

where Y_p^{υ} and Y_n^{υ} are the signal sequences of Y_p and Y_n in a segment υ of time length n with their corresponding local trends y_p^{υ} and y_n^{υ}, and $2L_n$ is the total number of the segments in the entire signal. The vectors $\vec{V}_p^{\upsilon}$ and $\vec{V}_n^{\upsilon}$ are the n-dimensional vectors that denote the local detrended signals $(Y_p^{\upsilon}-y_p^{\upsilon})$ and $(Y_n^{\upsilon}-y_n^{\upsilon})$ in the segment υ, respectively. The solid (dotted) lines in Figs. 1(a) and 1(c) represent the signals $x_p(t)$ $[x_n(t)]$ and $\vec{V}_p^{\upsilon}(t)$ $[\vec{V}_n^{\upsilon}(t)]$ in a segment υ, respectively. Here, FX data with time length n (=400) are used [8]. The solid horizontal line in Fig. 1(c) corresponds to the local trends $y_p^{\upsilon}(t)$ and $y_n^{\upsilon}(t)$. Figures 1(a) and 1(c) show that $\vec{V}_p^{\upsilon}(t)$ $[\vec{V}_n^{\upsilon}(t)]$ has the tendency to be positive (negative) in the time region with large magnitude fluctuations in $x_p(t)$ $[x_n(t)]$, and negative (positive) in the time region with small magnitude fluctuations. When the fluctuations in $x_p(t)$ and $x_n(t)$ increase and decrease synchronously, $\vec{V}_p^{\upsilon}(t)$ and $\vec{V}_n^{\upsilon}(t)$ have opposite signs. This relation is obvious because $Y_p(t)$ and $Y_n(t)$ are the cumulative integrated signals of $x_p(t)$ and $x_n(t)$, respectively. The term inside the large parenthes in the second equality of Eq. (2) represents a dot product between $\vec{V}_p^{\upsilon}$ and $\vec{V}_n^{\upsilon}$. When $x_p(t)$ and $|x_n(t)|$ increase or decrease synchronously on a time scale n, this dot product becomes negative with $\frac{\pi}{2}<\theta_{pn}^{\upsilon}<\pi$ [Figs. 1(a) and 1(c)]. It becomes positive with $0<\theta_{pn}^{\upsilon}<\frac{\pi}{2}$ for asynchronous increase or decrease in $x_p(t)$ and $|x_n(t)|$ [Figs. 1(b) and 1(d)]. The former case with $\frac{\pi}{2}<\theta_{pn}^{\upsilon}<\pi$ is defined as the out-of-phase correlation between the magnitude fluctuations of $x_p(t)$ and $x_n(t)$, and the other case with $0<\theta_{pn}^{\upsilon}<\frac{\pi}{2}$ is the in-phase correlation. Therefore, the function $F_{pn}(n)$ describes the time organization structure in correlation between the magnitude fluctuations $x_p(t)$ and $|x_n(t)|$, on a scale n.

In the DFA method, the function $F(n)$ is usually approximated by a power-law scaling function, so that we write

$$F^2(n) \sim k^2 n^{2H} \sim F_p^2(n) + F_n^2(n) + 2F_{pn}(n), \quad (3)$$

where the Hurst exponent H describes the correlation property of $x(t)$ [10]. When $H\sim 0.5$, the signal is uncorrelated. When $H<0.5$ (>0.5), the signal is anticorrelated (correlated). If $F_{pn}(n)<0$ (>0) for all scales n, the out-of-phase (in-phase) correlation between $x_p(t)$ and $|x_n(t)|$ is dominant. From this relation, the decomposition of the fluctuation function $F_{\|}(n)$ for the magnitude (or volatility) signal $|x(t)|$ can also be derived. The magnitude signal $|x(t)|$ can be expressed as $|x(t)|=x_p(t)+|x_n(t)|$. Therefore, the vector $\vec{V}_n^{\upsilon}$ in Eq. (2) is transformed into $-\vec{V}_n^{\upsilon}$ and for the three functions on the right hand side of Eq. (1) the function $F_{pn}(n)$ becomes $-F_{pn}(n)$ while the other functions remain unchanged. From Eqs. (2) and (3), it is straightforward to see that the fluctuation function $F_{\|}(n)$ can be written as

$$F_{\|}^2(n) \sim k_{\|}^2 n^{2H_{\|}} \sim F_p^2(n) + F_n^2(n) - 2F_{pn}(n), \quad (4)$$

where the new magnitude Hurst exponent $H_{\|}$ describes the correlation property of the magnitude signal $|x(t)|$. From Eqs. (3) and (4), we obtain

$$k_{\|}^2 n^{2H_{\|}} - k^2 n^{2H} = k_{\|}^2 n^{2H_{\|}}\left[1-\left(\frac{k}{k_{\|}}\right)^2 n^{2(H-H_{\|})}\right]$$
$$\sim -4F_{pn}(n)\,[=f_{pn}^2(n)]. \quad (5)$$

The difference between the scaling behavior (H) of $F(n)$ and scaling behavior $(H_{\|})$ of $F_{\|}(n)$ is induced by the time organization structure of the function $-4F_{pn}(n)$ for a scale n. The signal with volatility correlation behavior corresponds to $H_{\|}>0.5$ and $H\lesssim 0.5$. Since $H_{\|}>H$, $F_{pn}(n)$ in Eq. (5) is

dominated by the scaling behavior of $F_{\|}(n)$ as the scale n increases. In this case, from Eq. (5), we see that $F_{pn}(n)$ becomes negative (out of phase) for $n > n_{min}$, where the minimum scale n_{min} is given by

$$n_{min} \sim \left(\frac{k}{k_{\|}}\right)^{1/(H_{\|}-H)}. \tag{6}$$

In this scale region with out-of-phase correlation, the function $-4F_{pn}(n)$ in Eq. (5) is denoted as $f^2_{pn}(n)$ for convenience. Only this scaling region is studied for the analysis of the HRV data and FX data used in our paper. Note that, as $n \to \infty$, $f_{pn}(n)$ converges to the scaling behavior of $F_{\|}(n)$ with the exponent $H_{\|}$. The signal with the synchronous relation (out-of-phase correlation) between the magnitude fluctuations of positive and negative components can exhibit volatility correlation behavior.

B. Application to real data

We have applied our method to complex time series with volatility correlations. As typical examples, we chose heart rate variability and foreign exchange data [8]. We used the second-order detrended fluctuation analysis (DFA2) with scales $64 \leqslant n \leqslant 1024$. The scale n denotes the increments of heartbeat (RR) interval sequences, which are composed of the time durations between consecutive R waves of electrocardiograms, in the HRV data and logarithmic price changes in the FX signals [8]. In Fig. 2, both HRV and FX data show long-range correlation properties in their magnitude fluctuations with $H_{\|} > 0.5$. However, the original HRV signals are highly anticorrelated ($H \sim 0$), while the original FX signals are almost uncorrelated ($H \leqslant 0.5$). For the HRV data, the term kn^H in Eq. (5) becomes negligible in comparison with $k_{\|}n^{H_{\|}}$ for large n because $H(<H_{\|})$ approaches zero. Therefore, in Fig. 3(a), the function $f_{pn}(n)$ has scale invariance with the same scaling exponent ($H_{\|}$) as $F_{\|}(n)$ for all scales n. In Fig. 2(a), the scaling exponents H_{pn} (open circles) of $f_{pn}(n)$ are almost equal to those of $H_{\|}$ (closed circle) for the entire region in n. On the other hand, for the FX data, a universal scaling behavior of $f_{pn}(n)$ cannot be defined for all scales n because the exponent H is not negligible compared with $H_{\|}$ for the short-range scale n. For the long-range scale, $f_{pn}(n)$ approaches the scaling behavior of $F_{\|}(n)$ [Fig. 3(b)]. These empirical findings suggest that the relation between the correlation properties of the original signal and its magnitude can be explained through a correlation structure $[f_{pn}(n)]$ between fluctuation magnitudes of positive and negative components for the scale n.

III. MAGNITUDE CROSS-CORRELATION FUNCTION

We can study the nontrivial correlation structure between magnitude fluctuations of positive and negative components of a signal for a scale n by using the magnitude cross-correlation function. This magnitude cross-correlation function is defined by

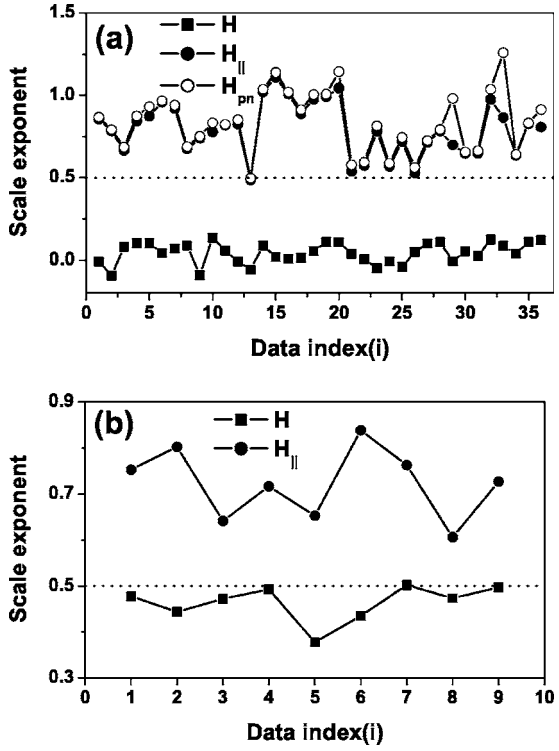

FIG. 2. (a) The scale exponents H, $H_{\|}$ (•), and H_{pn} (○) of the interbeat interval signals $x(t)$ for 36 HRV data. (b) The scale exponents H and $H_{\|}$ of price change signals $x(t)$ of nine foreign exchange rates for the U.S. dollar. Data indices: $i=1$ (Germany, DEM), 2 (Japan, JPY), 3 (Italy, ITL), 4 (France, FRF), 5 (Switzerland, CHF), 6 (Belgium, BEF), 7 (Denmark, DKK), 8 (Spain, ESP), and 9 (Finland, FIM).

$$C(n;\Delta Y_p(n,t),|\Delta Y_n(n,t)|) = \frac{\langle \Delta Y_p|\Delta Y_n|\rangle - \langle \Delta Y_p\rangle\langle|\Delta Y_n|\rangle}{\sigma_{\Delta Y_p}\sigma_{\Delta Y_n}}, \tag{7}$$

where $\Delta Y_p(n,t) = Y_p(t+n) - Y_p(t)$ and $\Delta Y_n(n,t) = Y_n(t+n) - Y_n(t)$ $(t=1,2,\ldots,N-n)$. The quantities $\sigma_{\Delta Y_p}$ and $\sigma_{\Delta Y_n}$ correspond to the standard deviations of ΔY_p and ΔY_n, respectively. The signal $\Delta Y_p(n,t)$ $[|\Delta Y_n(n,t)|]$ is given by $\Sigma_{i=t+1}^{t+n} x_p(i)$ $[\Sigma_{i=t+1}^{t+n}|x_n(i)|]$, which represents the volatility of a positive (negative) component for a given scale n. Therefore, the magnitude cross-correlation function $C(n;\Delta Y_p,|\Delta Y_n|)$ exhibits the correlation structure between the magnitude fluctuations of positive and negative components of a signal $x(t)$ for a given scale n. The magnitude cross-correlation function ranges between -1 and 1. It approaches 1 (-1) faster as the out-of-phase (in-phase) correlation structure in a signal becomes more dominant for a scale n.

Figure 4(a) shows the magnitude cross-correlation function $C(n)$ for HRV signals of five people randomly selected from 36 data sets in Fig. 2(a). We find that the HRV signals are highly out-of-phase correlated for all scales with $C(n) > 0.95$. In Fig. 4(b), $C(n)$ for five FX data [index $i=1-5$ in Fig. 2(b)] are plotted and compared with those for the HRV data in Fig. 4(a). We can see that the $C(n)$ of HRV data approaches unity much faster than that of the FX data,

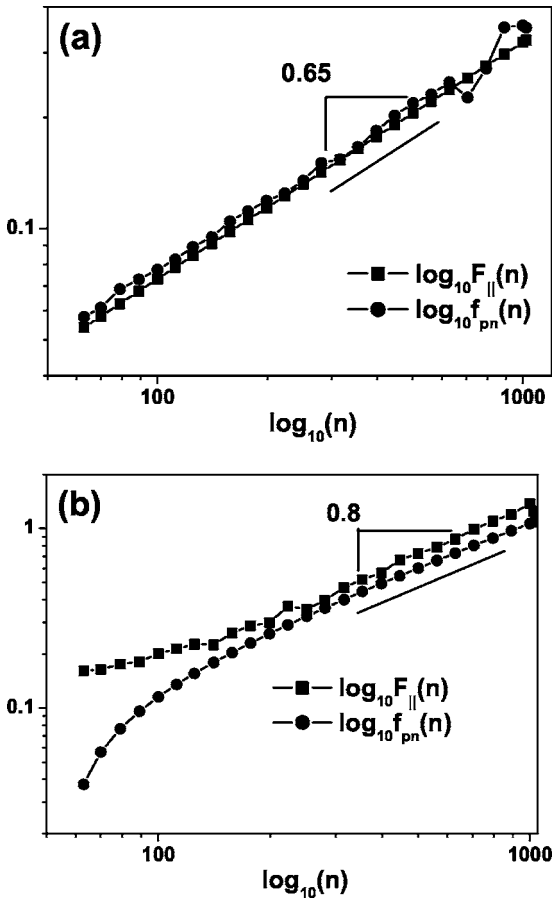

FIG. 3. (a) The scaling behaviors of $F_{\|}(n)$ (■) and $f_{pn}(n)$ (●) for the HRV signal of a healthy subject [8]. (b) The scaling behaviors of $F_{\|}(n)$ and $f_{pn}(n)$ for the JPY-USD FX data in Fig. 2(b).

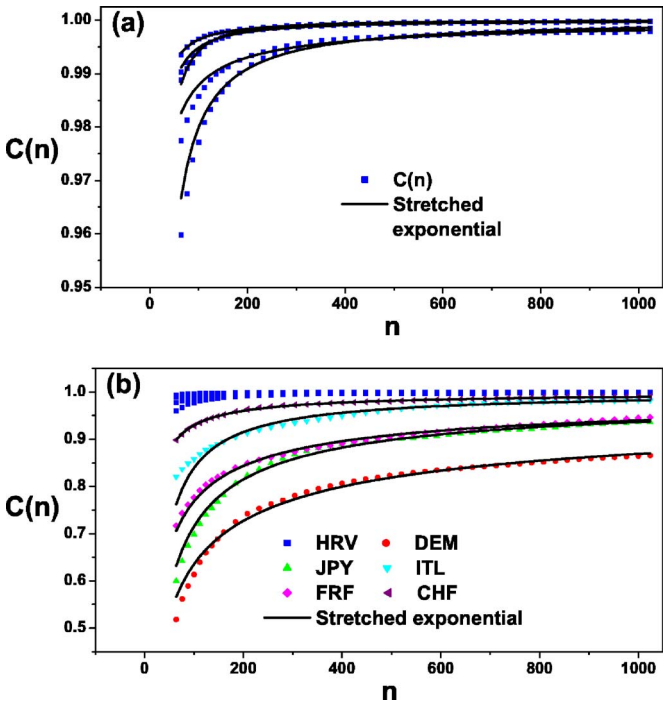

FIG. 4. (Color online) (a) The magnitude cross-correlation function $C(n)$ for five people randomly selected from the 36 HRV data. The function $C(n)$ is fitted by a stretched-exponential function (solid curves). (b) The function $C(n)$ (square dotted) of HRV data in Fig. 4(a) is plotted for comparison with $C(n)$ of FX data.

which suggest that the HRV signals are more anticorrelated than the FX signals (Fig. 2). The correlation functions $C(n)$ in Figs. 4(a) and 4(b) are fitted by a stretched exponential-function (continuous curves) [7]

$$C(n) \sim \exp\left[-\left(\frac{n}{T}\right)^{\gamma}\right] \quad (\gamma < 0), \tag{8}$$

where T is constant. The correlation function in [7] is a stretched-exponentially decaying function since $0<\gamma<1$. However, in our case, it is an increasing function since $\gamma<0$. By rescaling Eq. (8), we get

$$R(n) = T[-\ln C(n)]^{1/\gamma} \sim n. \tag{9}$$

Figure 5(a) shows that the relation in Eq. (9) is satisfied for both HRV and FX signals and the function $C(n)$ is fitted by a stretched-exponential function very well. Due to the form of the stretched-exponential function in Eq. (8), $C(n)$ approaches unity faster as γ and T decrease further. Therefore, the original signal becomes more anticorrelated as γ and T decrease. Figure 5(b) shows γ and T derived from the magnitude cross-correlation function $C(n)$ of the HRV and FX signals. The dissimilarity between the characteristic behaviors of $C(n)$ of HRV and FX data is well classified by the line of $\gamma=-1$. The magnitude signals of HRV and FX data have similar long-range correlation properties as in Fig. 2. However, due to this dissimilarity in γ and T the original signals of HRV data are highly anticorrelated ($H\sim 0$), while the FX data are almost uncorrelated ($H\lesssim 0.5$). In general, signals with identical long-range correlations in their magnitude signals can exhibit different correlation properties depending on the structure of the function $C(n)$ defined by γ and T.

IV. THE NONLINEAR TIME ORGANIZATION STRUCTURE OF FUNCTION $C(n)$

Here, we investigate the nonlinear property of the function $C(n)$ through the surrogate test. It has been shown that the long-range correlation property of the magnitude fluctuations carries information on the nonlinear properties of the original signals (heartbeat or multifractal signals) [3,4]. In Eq. (5), the exponent H reflects the linear two-point correlation structure; thus the nonlinear property of the magnitude fluctuation can be embedded into the time organization of $F_{pn}(n)$. We generate surrogate data for the HRV and FX data in Fig. 4(b) by randomizing the Fourier phases of these data, preserving the amplitude of the Fourier transform. This procedure eliminates nonlinearities, preserving linear features (H) of the original signals [11]. Figure 6 shows the behaviors of $C(n)$ for the original and surrogate signals of HRV [Fig. 6(a)] and FX [Fig. 6(b)] data. The structures of $C(n)$ of the original signals are destroyed by the surrogate procedure, while those of the surrogate signals exhibit time organization significantly different from the stretched-exponential func-

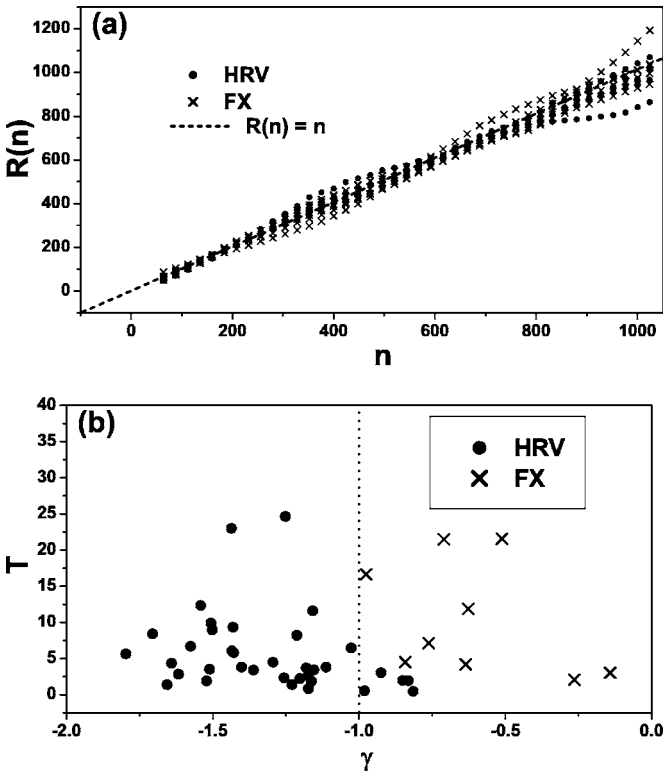

FIG. 5. (a) The rescaled functions $R(n)$ in Eq. (9) for the HRV (●) and FX (×) data in Figs. 4(a) and 4(b), respectively. (b) The distribution of γ and T for the magnitude cross-correlation $C(n)$ of 36 HRV data (●) and nine FX data (×).

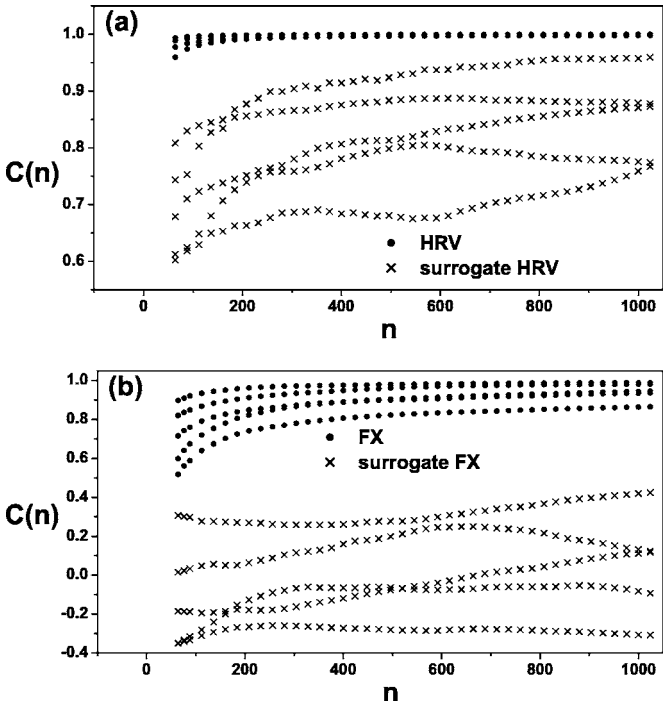

FIG. 6. (a) The functions $C(n)$ (●) for $x(t)$'s of five HRV data in Fig. 3(a) and (×) for $x(t)$'s of their surrogate data. (b) The function $C(n)$ (●) for $x(t)$'s of five FX data in Fig. 3(b) and (×) for $x(t)$'s of their surrogate data.

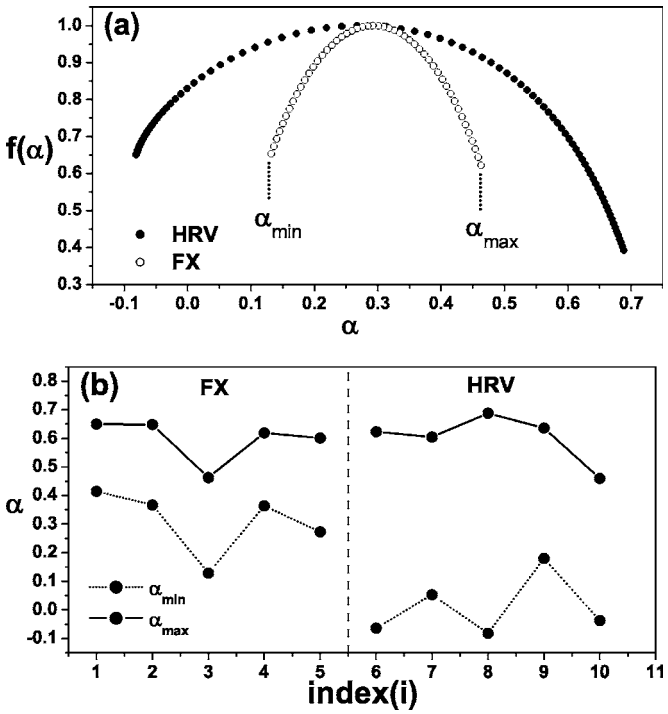

FIG. 7. (a) The multifractal spectrum for the typical HRV (●) and FX (○) data. (b) The minimum α (dotted line) and the maximum α (solid line) in the α-$f(\alpha)$ curve for FX ($i=1-5$) and HRV ($i=6-10$) data.

tion in Eq. (8). Our result shows that the time organization in the correlation between magnitude fluctuation signals of positive and negative components is related to the nonlinear properties of these HRV and FX signals.

V. THE MULTIFRACTAL ANALYSIS

Ashkenazy *et al.* demonstrated that the difference between the correlation properties of the original signal and its magnitude signal is proportional to the multifractal spectrum width for signals generated by the multiplicative cascading process and real finance data [4]. In our result, the relation between the correlation properties of the original and magnitude signals is connected to the behavior of the correlation function $C(n)$ for the scale n, which, in turn, is related to the multifractal structure of the original signal.

We derive the multifractal spectrum for the HRV data in Fig. 4(a) and the FX data in Fig. 4(b). Figure 7(a) represents the multifractal structures for typical HRV data and FX data. We applied the wavelet transform modulus maxima (WTMM) method to derive the multifractal spectrum with the local Hurst exponent α and the function $f(\alpha)$ [12]. The function $f(\alpha)$ is the fractal dimension of the subset of the time series characterized by the local Hurst exponent α. The multifractal spectrum width in the α-$f(\alpha)$ curve in Fig. 7(a) reflects the nonlinear features of time series characterized by diverse local Hurst exponents [2,4]. The width is defined by the difference ($\Delta\alpha$) between the minimum Hurst exponent (α_{min}) and the maximum Hurst exponent (α_{max}) in Fig. 7(a). Figure 7(b) shows α_{min} and α_{max} for the FX (index $i=1-5$)

and HRV ($i=6-10$) data in Fig. 4, respectively. We can see that the width $\Delta\alpha$ ($=0.28\pm0.04$) of the FX data is much narrower than $\Delta\alpha$ ($=0.59\pm0.13$) of the HRV data.

VI. CONCLUSION

In summary, we have provided the basic relation between the correlation properties of the original signal and its magnitude fluctuation from the superposition rule of the DFA method. The relation can be explained by the time organization structure in the correlation between the fluctuation of the magnitude of the positive and negative components of the original signal. We have proposed the magnitude cross-correlation function $C(n)$ to show the nontrivial correlation structure between these two component signals for empirical HRV and FX data. Moreover, signals $x(t)$ with identical long-range correlations $H_{\|}$ in their magnitude fluctuations can exhibit different time organizations H depending on the behavior of the magnitude cross-correlation function $C(n)$ for the scale n. Our method can be applied to elaborate correlation analysis and classification of diverse complex signals including medical, economic, and climatic signals. In particular, stochastic models such as long-memory stochastic volatility and fractionally integrated GARCH (FIGARCH), which allows for long memory in the conditional variance of price changes [13], in econometrics treat the long-memory property in absolute returns of price data with short-range correlation. Those need to be tuned to reflect the time organization structure of the magnitude cross-correlation function.

ACKNOWLEDGMENTS

We thank Olsen and Associates for the use of foreign exchange data. This work was supported by the Ministry of Science and Technology and the Ministry of Education and Human Resources of Korea.

[1] R. N. Mantegna and H. E. Stanley, *An Introduction to Econophysics: Correlation and Complexity in Finance* (Cambridge University Press, Cambridge, U.K., 1999); J-P. Bouchaud, A. Matacz, and M. Potters, Phys. Rev. Lett. **87**, 228701 (2001).

[2] P. C. Ivanov *et al.*, Nature (London) **399**, 461 (1999); R. B. Govindan and H. Kantz, Europhys. Lett. **68**, 184 (2004); A. Bunde, J. F. Eichner, J. W. Kantelhardt, and S. Havlin, Phys. Rev. Lett. **94**, 048701 (2005).

[3] Y. Ashkenazy *et al.*, Phys. Rev. Lett. **86**, 1900 (2001).

[4] Y. Ashkenazy *et al.*, Physica A **323**, 19 (2003); K. Matia, Y. Ashkenazy, and H. E. Stanley, Europhys. Lett. **61**, 422 (2003).

[5] T. Kalisky, Y. Ashkenazy, and S. Havlin, Phys. Rev. E **72**, 011913 (2005); B. Podobnik *et al.*, *ibid.* **72**, 026121 (2005).

[6] C.-K. Peng *et al.*, Phys. Rev. E **49**, 1685 (1994).

[7] E. W. Montroll and J. T. Bendler, J. Stat. Phys. **34**, 129 (1984); R. V. Chamberlin, G. Mozurkewich, and R. Orbach, Phys. Rev. Lett. **52**, 867 (1984); J. Klafter and M. F. Shlesinger, Proc. Natl. Acad. Sci. U.S.A. **83**, 848 (1986).

[8] The HRV data, available at http://www.physionet.org/physiobank/, include heartbeat (RR) interval signals for 21 healthy and 15 unhealthy (congestive heart failure) individuals, each with 15 000 data points. We focus on the heartbeat interval increment signals generated from these data. The FX data are from Olsen and Associates with nine global spot FX rates [Fig. 2(b)]. The data run from 1 Janvary 1996 to 31 December 1996 with 12 524 records at half-hour intervals. We used the logarithmic price change signals.

[9] K. Hu, P. C. Ivanov, Z. Chen, P. Carpena, and H. E. Stanley, Phys. Rev. E **64**, 011114 (2001); Z. Chen, P. C. Ivanov, K. Hu and H. E. Stanley, *ibid.* **65**, 041107 (2002).

[10] Jens Feder, *Fractals* (Plenum Press, New York, 1988).

[11] J. Theiler *et al.*, Physica D **58**, 77 (1992).

[12] J. F. Muzy, E. Bacry, and A. Arneodo, Int. J. Bifurcation Chaos Appl. Sci. Eng. **4**, 245 (1994).

[13] R. T. Baillie, J. Econometr. **73**, 5 (1996); R. F. Engle, *ARCH: Selected Readings* (Oxford University Press, Oxford, 2000).